Title

The Quest for Accurate Liquid Water Properties from First Principles

Journal

The Journal of Physical Chemistry Letters, 9(17)

ISSN

1948-7185

Authors

Pestana, Luis Ruiz

Marsalek, Ondrej

Markland, Thomas E

et al.

Publication Date

2018-09-06

DOI

10.1021/acs.jpclett.8b02400

Peer reviewed

The Quest for Accurate Liquid Water Properties from First Principles

Luis Ruiz Pestana[1,2], Ondrej Marsalek[3], Thomas E. Markland[4], and Teresa Head-Gordon[1, 2, 5, 6, 7*]
[1]Chem. Sci.s Division, Lawrence Berkeley National Laboratory and [2]Pitzer Center for Theoretical Chemistry, University of California, Berkeley CA 94720
[3]Charles University, Faculty of Mathematics and Physics, Ke Karlovu 3, 121 16 Prague 2, Czech Republic
[4]Department of Chemistry, Stanford University, Stanford, California 94305, USA
[5]Department of Chemistry, [6]Department of Bioengineering, [7]Department of Chemical and Biomolecular Engineering, University of California, Berkeley CA 94720

Developing accurate *ab initio* molecular dynamics (AIMD) models that capture both electronic reorganization and nuclear quantum effects associated with hydrogen bonding is key to quantitative understanding of bulk water and its anomalies, as well as its role as a universal solvent. For condensed phase simulations, AIMD has typically relied on the generalized gradient approximation (GGA) of Density Functional Theory (DFT) as the underlying model chemistry for the potential energy surface, with nuclear quantum effects (NQEs) sometimes modeled by performing classical molecular dynamics simulations at elevated temperatures. Here we show that the properties of liquid water obtained from the meta-GGA B97M-rV functional, when evaluated using accelerated path integral molecular dynamics simulations, displays accuracy comparable to a computationally expensive dispersion corrected hybrid functional, revPBE0-D3. We show that the meta-GGA DFT reproduces bulk water properties including radial distribution functions, self-diffusion coefficients, and infrared (IR) spectra with comparable accuracy of a much more expensive hybrid functional. This work demonstrates that the underlying quality of a good DFT functional requires evaluation with quantum nuclei, and that high temperature simulations are a poor proxy for properly treating nuclear quantum effects.

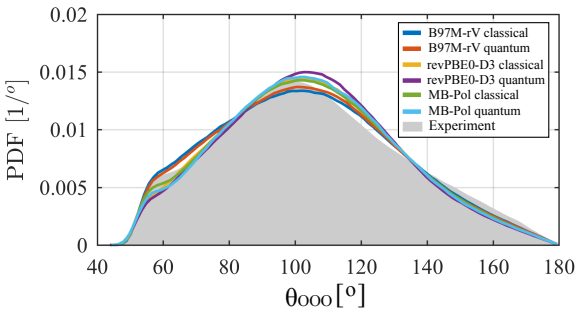

*corresponding author

For close to 50 years some of the most successful models for liquid water have been based on empirical functional forms that capture the electronic structure and nuclear quantized motions implicitly through their parameterization using condensed phase data.[1] While this usually provides good accuracy of water properties near regions of phase space where the model is parameterized, it often comes at the expense of transferability to other state points or for solvation studies.[1] However, the ultimate goal of this field is to create general theoretical models that are transferable, predictive, and at the most challenging, able to describe chemically reactive systems.

Over the last 20 years, a highly promising approach for achieving all of these goals has been advanced through *ab initio* molecular dynamics (AIMD) simulations, where the nuclei are evolved based on the interactions between the atoms calculated on the fly from the instantaneous electronic structure of the system. In the condensed phase, for which sampling the statistically relevant configurations of the system is just as important as the quality of the underlying potential energy surface, AIMD has almost exclusively relied on the relatively inexpensive Kohn-Sham Density Functional Theory (DFT)[2-10], although some studies using the MP2 wavefunction method have been reported[11-12]. Since in AIMD simulations the nuclei evolve on the bare Born Oppenheimer potential energy surface, nuclear quantum effects (NQEs) cannot be taken into account implicitly and have to be treated explicitly. Water is typically the first test bed for new models and methods due to its small molecular size, the relative simplicity of its covalent structure, but also because of its inherently interesting anomalous properties that arise from complex intermolecular interactions as an associated liquid.

For DFT, the approximation to the exchange-correlation functional can be organized into a hierarchy of increasing accuracy according to a "Jacob's ladder" of complexity. The lowest rung is comprised of the local density approximation (LDA), which is greatly improved upon at the second rung by the generalized gradient approximation (GGA), such that the latter has dominated simulations of liquid water to date. The simulated properties of liquid water using early GGA functionals such as Becke-Lee-Yang-Parr (BLYP)[13-14] or Perdew-Burke-Ernezerhof (PBE)[15] are now well-known, in which water was found to be overstructured and glassy at ambient temperature and pressure[7, 9, 16-18]. This failure is largely due to the well-known delocalization or self-interaction error[19], which leads to systematic red shifted errors in the monomer deformability[10] and thus systematic overbinding when analyzed on dimer data sets[20-21].

This is made even more severe when also accounting for NQEs, since these add the equivalent of ~5 kcal/mol of extra zero-point energy into the O-H coordinate, thus providing even more propensity to delocalize the proton in the hydrogen bond.[22] This is one reason perhaps why NQEs are typically neglected altogether in the evaluation of liquid water AIMD simulations using standard GGA density functionals, because they appear to work well without them included.[4, 6] The neglect of NQE has also been a practical consideration, since conventional path-integral methods are about two orders of magnitude more computationally expensive than simulations where the nuclei are treated classically. It is the latter especially that has led to an *ad hoc* model for NQEs, which is to run the classical dynamics at a higher temperature (and sometimes at negative pressure) to mimic an aspect of NQEs, which is the delocalization of the proton and weakening of the hydrogen-bonded network.

Since this early pioneering work, improved physics and computational methods have advanced on several fronts. First is the inclusion of simple and practical non-local dispersion corrections such as DFT-D[23-24], (r)VV10[25-26], vdW-DF[27], or the Tkatchenko and Scheffler vdW[28-29]. The accounting for non-local dispersion is known to counteract the overstructuring of liquid water by GGA functionals.[9, 30]. The second is the investigation of DFT functionals that are classified on higher rungs of Jacobs ladder than GGAs, such as hybrid and double hybrid functionals at rungs four and five, in which the Hamiltonian is a fully nonlocal operator due to inclusion of some percentage of exact exchange[4, 8]. The self-interaction problem in DFT is known to also be mitigated by including exact exchange in the density functional, and thus to significantly improve the description of water's bond deformation energies.[31] Finally, new methods such as the ab initio ring polymer contraction (AI-RPC) approach[22], combined with multi-time scale (MTS) propagation[32] and appropriate thermostats[33], allows for accurate inclusion of NQEs in AIMD calculations at a significantly reduced cost.[34] The ability to now simulate NQEs much more reliably and cheaply[22, 34] offers the opportunity to assess the ad hoc estimator of NQEs (if they are estimated at all) comprised of a classical trajectory run at an elevated temperature[5, 35].

To illustrate the interplay of all three advances, the current snapshot of progress on simulating liquid water from first principles is that the hybrid non-empirical functional revPBE0 that includes the empirical D3 dispersion correction (revPBE0-D3) and simulated with NQEs, shows very good agreement with bulk phase experimental properties at ambient conditions.[4] This in turn has informed the fact that while dispersion-corrected GGA models such as revPBE-D3

show good agreement with many water properties using classical dynamics[6, 35], it arises from a fortuitous cancellation of errors in which the neglect of exact exchange counterbalances the neglect of quantum nuclei[4]. This leaves the AIMD field for liquid water and solvation studies facing a computationally painful prospect of needing to include exact exchange at roughly two orders of magnitude the cost of a GGA functional to get liquid properties and/or their trend with temperature and pressure that is reliable.

A number of *ab initio* studies on liquid water have attempted to reproduce basic experimental water properties using approximate density functionals and classical trajectories, in some cases artificially raising or lowering the temperature to mimic the effects of NQEs. The question is how much correct physics is required to declare true victory in a model chemistry for liquid water and its role as an aqueous solvent? Considering the history of AIMD simulations, what likely matters for an accurate description of bulk water is not whether exact exchange must be included, or whether it is dressed with an additive dispersion term, but that a well-optimized DFT functional should be balanced among interactions so as to accurately describe water covalent bonds and their deformability. In turn, an accurate potential energy surface for the water monomer is necessary for an accurate description of intermolecular hydrogen-bonding[31], thereby allowing for nuclear quantum effects to operate effectively for describing the proton dynamics. In this study we examine this balance for the semi-local meta-GGA functional B97M-rV that builds in the non-local correlation VV10 functional into the fitting procedure[36-38] in order to compare it against the established hybrid GGA functional revPBE0-D3 for liquid water[24]. In addition, we perform 200 ps simulations for the meta-GGA functional using thermostatted ring polymer molecular dynamics (TRPMD) to compare its properties against a classical simulation at an elevated temperature of 330K.

Figure 1 shows the intermolecular radial distribution functions (RDFs) for oxygen-oxygen $g_{OO}(r)$, hydrogen-hydrogen $g_{HH}(r)$, and oxygen-hydrogen $g_{OH}(r)$, comparing the meta-GGA and hybrid functional simulated with classical and quantum nuclei, and compared against experimental data[39-40]. Under classical dynamics, the meta-GGA functional is in very good agreement with the hybrid GGA functional and with the experimental data, although the meta-GGA slightly underestimates the second peak and overestimates the intensity in the interstitial region, which is evidence of lower tetrahedrality. The addition of NQEs moves the DFT models more closely to

the experimental values for the RDFs involving hydrogen and thus yield small improvements in the $g_{OO}(r)$ as well.

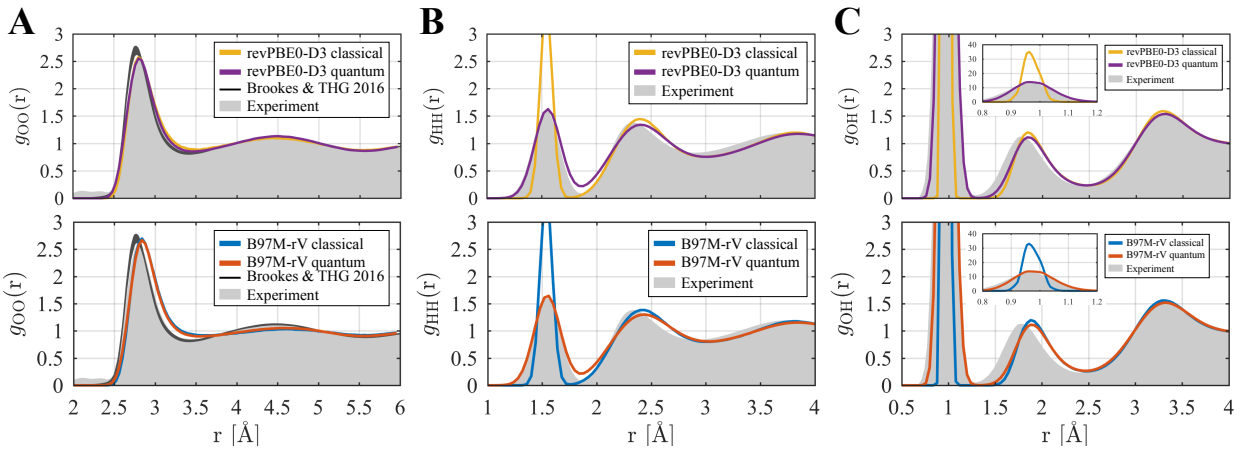

Figure 1. *Water radial distribution functions (RDF) using either classical or quantum dynamics for B97M-rV and the previously published revPBE0-D3 results*[4]. (A) $g_{OO}(r)$, (B) $g_{HH}(r)$, and (C) $g_{OH}(r)$. AIMD simulations of water performed at the experimental bulk liquid density at 300 K. The experimental data is shown as gray shade for reference.[39-40] The additional curves in black eliminates the unphysical density at low r and conforms to the isothermal compressibility that overcomes problems with the original experimental analysis.[41]

Both functionals are slightly too incompressible due to shifting of the first peak position out to higher values of r.[41] It is possible that the finite Gaussian basis set using TZV2P (see Methods) and the plane wave cutoffs used in AIMD are also contributing to this disagreement. In previous work we examined the errors introduced with a small plane wave cutoff and small basis for the binding energies of the S22 data set, and binding and isomerization energies for WATER20 data sets.[3] In particular we benchmarked CP2K using the mDZVP and mTZV2P basis sets, and plane wave cutoffs of 400 Ry and 800 Ry, and compared them to all electron calculations using a def2-QZVPPD basis set evaluated with fine grids.[3] We found that the B97M-rV functional overbinds by 1-2%, and the isomerization energy errors were very small under the standard AIMD simulation conditions.[3] Furthermore, we also compared the classical MD structure for liquid water using the smaller TZV2P basis set (the one used here) and find that we get very close to the same result when using the larger MOLOPT mTZV2P basis set reported previously (see Figure S1). It is noteworthy that a similar NQE study of the SCAN+rVV10 meta-GGA functional[42] found that the structural properties of liquid water were significantly overstructured and in relatively poor agreement with experiment compared to the two functionals examined here.[43] Overall this appears

to be due to the fact that the bare SCAN functional[44] significantly overbinds in general, the addition of rVV10 makes the overbinding worse, and the AIMD simulation conditions likely exacerbates this further.[38]

Figure 2 presents a comparison of the functionals on the two different rungs, and the differences due to classical vs. nuclear quantum dynamics, on the complementary set of probability distributions that probe different features of the hydrogen-bonding network, including: the covalent bond length d_{OH}, hydrogen bonding angle θ defined by the O_D- H_D-O_A vertices, proton transfer coordinate $\delta = d_{O_DH_D} - d_{O_AH_D}$, as well as for the molecular dipole μ. Under classical dynamics, the hybrid functional shows a slightly shorter covalent bond (Figure 2A) greater linearity of the hydrogen-bond (Figure 2B), and a larger molecular dipole moment (Figure 2D) which aligns with the RDF profiles in that revPBE0-D3 is slightly more structured overall compared to the meta-GGA.

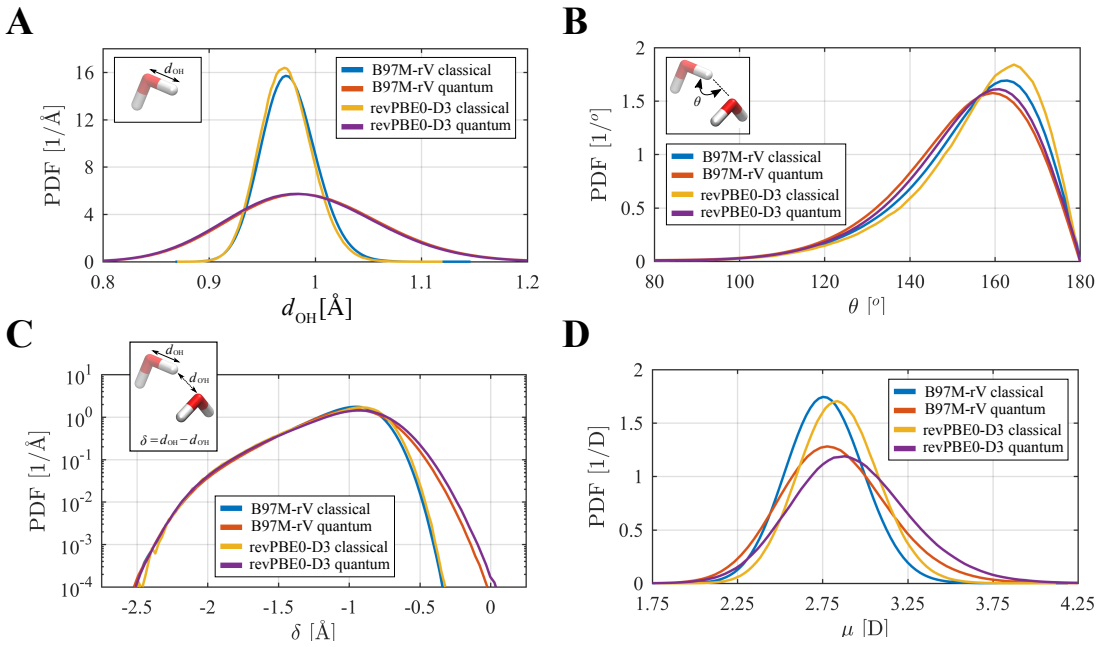

Figure 2. *Analysis of the hydrogen bond network using either classical or quantum dynamics for B97M-rV and revPBE0-D3* [4]. Shown are the probability density functions (PDFs) of: (A) covalent bond length, d_{OH}, (B) hydrogen bond angle θ, (C) proton transfer coordinate, δ, on semilogarithmic scale, and (D) molecular dipole μ. The insets illustrate the definition of d_{OH} and δ and θ.

However, Figure 2 makes clear that the differences in the underlying performance of the functionals is negligible compared to the influence of treating the nuclei quantum mechanically, which changes the hydrogen-bonding network fundamentally. In addition to the broadening of

these distributions due to proton delocalization, there is now non-zero probability of $\delta > 0$ (Figure 2C), indicating the presence of transient autoprotolysis.[45] It is interesting to see the competing effects introduced by the nuclear quantum effects[46], where proton delocalization along the covalent bond tends to strengthen hydrogen bonds, but while also slightly bending the hydrogen-bonds to being less linear. These competing effects are finely balanced at 300K[46] and thus give rise to the rather small changes in the RDFs when comparing the classical vs. quantum dynamical averaging in Figure 1.

Figure 3 continues the trend that the underlying differences between the two functionals are small relative to the (approximate) TRPMD treatment of the nuclear motions for the dynamical properties such as the IR spectra (Figure 3A) and self-diffusion coefficient (Figure 3B). For the calculated classical IR spectra, B97M-rV and revPBE0-D3 exhibit blue shifts of ~200 cm^{-1} and ~50 cm^{-1} for the stretching and bending mode, respectively, as well as low frequency librational modes that are red-shifted by ~80 cm^{-1}, indicating that the intermolecular hydrogen bonding network has somewhat more extensive rocking motions. However, the NQEs correct both functionals so that their peak positions better align with the peaks of the experimental IR spectra[47], with high frequency red shifts and low frequency blue shifts both consistent with the greater degree of proton delocalization. We note that the broadening of the peaks is an artifact of the approximate nature of the TRPMD, which has been seen previously[4, 48], as opposed to the underlying accuracy of the functionals themselves. In addition, both functionals show overall excellent agreement with the self-diffusion coefficient, which are within error bar of the experimental value[49], although the NQE has the opposite effect on the water self-diffusivity for the two functionals. It is not straightforward to explain this trend given the interplay between the functional and the proton delocalization promoted by NQEs, but nonetheless the effect is small compared to the error bars on the diffusion constant.

It has already been established that the revPBE-D3 GGA functional simulated with classical dynamics benefits from a cancellation of errors, i.e. the electronic model deficiencies cancel the neglect of NQEs at room temperature.[3-4] By contrast, excellent DFT functionals may at first appear to be inferior for dynamics using classical trajectories when in fact their better underlying electronic structure requires their accompaniment with appropriately described nuclear quantum effects.[3-4] For a long time, the problem of simulating nuclear quantum effects has been so exorbitantly expensive that a simpler approach has been taken in which the water system is

heated up to ~330K to mimic the disordering that might be engendered through delocalization of the proton. However, the proton fluctuations when accounted for with good estimate of quantum dynamics in actuality can give rise to not only this disordering feature but also some increase in the strengthening of directional hydrogen bonding – the latter effect that will not be captured at higher temperatures since the distribution of hydrogen bonding geometries have become more bent and thus are weaker on average.

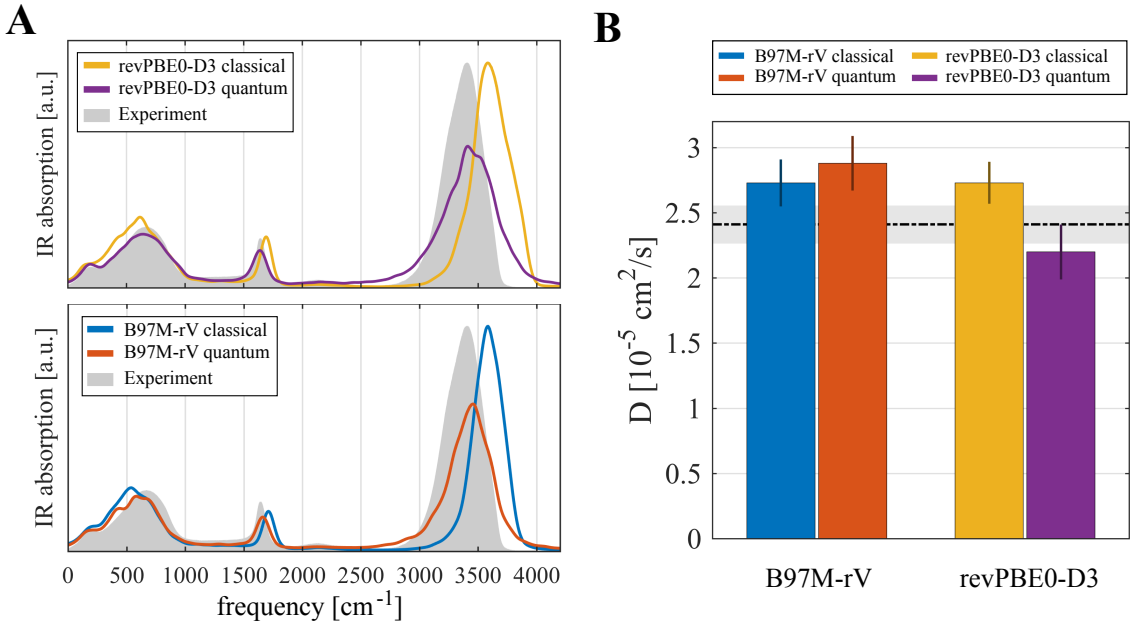

Figure 3. *Dynamical properties using either classical or quantum dynamics for revPBE0-D3* [4] *(top) and B97M-rV (bottom)*. (A) Infrared absorption spectrum and (B) the self-diffusion coefficient. The error bars in the self-diffusion coefficient correspond to the standard error of the diffusion coefficients when splitting the independent trajectories into segments of 25 ps; the diffusivity values from the simulations have been corrected for finite size effects. The experimental IR[47] and diffusion[49] data is shown as gray shade for reference.

To illustrate this point, Figure 4 shows a comparison of difference properties for structure and dynamics when trajectories are simulated using AIMD at 330K vs. the approximate but proper treatment using TRPMD simulations at 300K for B97M-rV, revPBE0-D3, as well as an accurate non-reactive model such as MB-pol model for yet an additional comparison. (The full results for all properties using the MB-pol model are given in Figures S2-S4). Overall the effects of temperature on a classical trajectory of a DFT functional or many-body model are *qualitatively* different than found from a quantum dynamical simulation. As might be expected, the effect of temperature on structural properties is to decrease the first shell coordination number and

tetrahedral signatures, and increase diffusion coefficients, seriously diminishing the agreement of these highly accurate *ab initio* models with experiment. Furthermore, increasing temperature has little effect on the high frequency vibrations calculated given the classical equipartition of the energy, whereas the quantum dynamics shows large red shifts that bring them into excellent alignment with the experimental IR peaks. For the non-reactive model MB-pol, properties degrade at low temperature when the equations of motion are simulated classically as recently shown.[50] This result is amplified in Figure 4 which shows the same qualitative trend in the degradation of properties using 330 K classical simulations of MB-pol to replicate the effect of including NQEs at room temperature.

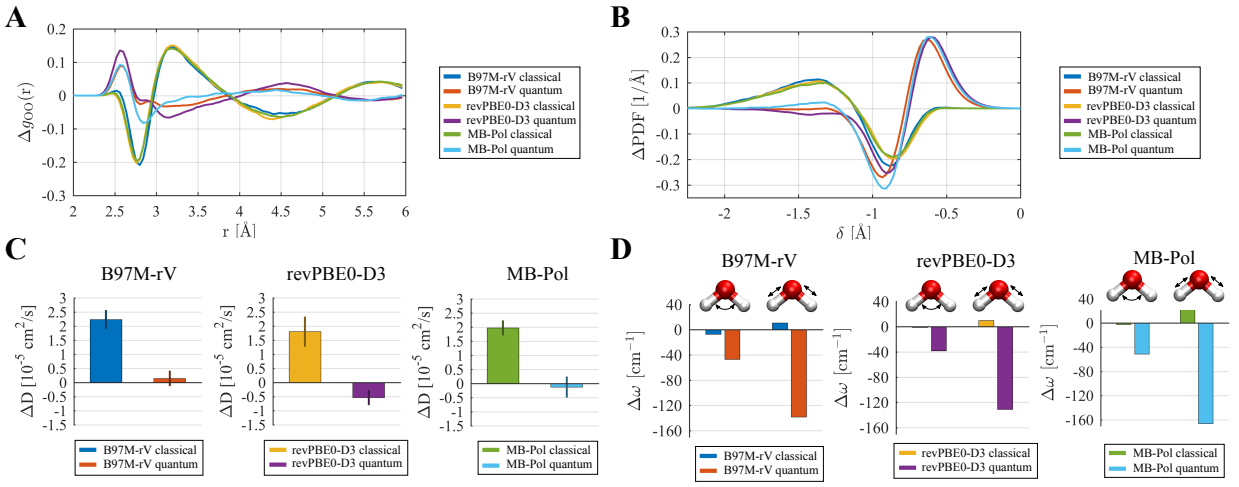

Figure 4. *Differences between the classical AIMD at 300 K reference state and either classical AIMD at 330 K or TRPMD simulations at 300K.* Differences are calculated for B97Mr-V and revPBE0-D3 for (A) oxygen-oxygen radial distribution function; (B) probability density of the proton transfer coordinate; (C) water self-diffusion coefficient; (D) Shifts in the hydrogen VDOS peaks corresponding to bending and stretching modes; negative values correspond to red shifts with respect to the classical AIMD simulations at 300 K.

But more is still required from theory in the quest for describing liquid water from first principles. We note that most AIMD studies, including this one, enforce the experimental value of the density of 0.997 g/cm^3, although the equilibrium density of water for the functional at hand may not correspond to ambient water. The accurate calculation of the equilibrium density remains challenging however, mainly due to large thermodynamic fluctuations in pressure associated with the small system sizes amenable to AIMD simulations and the requirement of larger plane-wave

cutoffs to achieve convergence in simulations in isobaric ensembles.[18, 51] The effects that NQEs have on the equilibrium density of the system are not well understood either, although recently reported AIMD results of the SCAN-rVV10[42] functional that has been simulated with NQEs using methodology that is similar to that reported here estimate an equilibrium density that is too high[43].

In summary, this work has established that a much less expensive meta-GGA semi-empirical functional B97M-rV, when combined with accelerated path integral simulations, is an excellent performer for reproducing ambient water properties at fixed density, and requires no temperature adjustments to represent the ambient liquid state correctly. The salient lessons from this study are multi-fold in regards DFT and NQEs when applied to liquid water. The first is that a meta-GGA functional on a lower rung of Jacob's ladder can exhibit equivalent quality to a hybrid functional.[38] Second, and as demonstrated previously[4], longer ~200 ps quantum trajectories are required to converge the range of basic water properties considered here; while water structure converges quite quickly (tens of picoseconds), the diffusive dynamics converge on a longer timescale. Finally, raising the temperature to "mimic" NQEs is an unambiguously poor approximation since the classical equipartition of energy among all dynamical modes of the system does not capture the true frequency dependence of the zero-point energy. This props the door open for more advanced chemical reactivity applications in water solvent that are currently too difficult to reach with the higher rungs of Jacobs ladder that incorporate exact exchange.

METHODS

We performed classical and path integral *ab initio* molecular dynamics (AIMD) simulations in the NVT ensemble of a system with 64 water molecules in a periodic cubic box of a 12.42 Å side (i.e. density of bulk water). Classical simulations were performed at two different temperatures, 300 K and 330 K, and path integral simulations at 300 K. The i-PI program[52] was used to propagate the nuclei with a multi time stepping (MTS) integrator as described in previous work[53] while forces were evaluated using the CP2K program [54]. We use a TZV2P basis set to expand the Kohn-Sham orbitals, and a cutoff of 400 Ry to represent the electron density in an auxiliary plane-wave basis. The electronic gradient tolerance in the self-consistent cycle was set to 5×10^{-7}.

Within the MTS scheme for both types of treatment of the nuclear motion, we calculate the reference forces at the SCC-DFTB[55] level of theory with Ewald summation used to evaluate long-range electrostatic and D3 dispersion corrections added[56]. The full forces are calculated using

Kohn-Sham DFT[57] using the Gaussian and plane waves (GPW) approach[58] implemented in the QUICKSTEP module[59] of CP2K. In this work, we are primarily testing the B97M-rV meta-GGA density functional[36-37]; it has been parameterized including the non-local correlation functional rVV10 with parameters b = 6.0 and C = 0.01[36-37]. We use the Goedecker-Teter-Hutter (GTH) pseudopotentials optimized for the functional PBE to represent the core electrons. We recently showed that the pseudopotentials, even when they are not functional-optimized, introduce a very small error with respect to reference all-electron calculations. For the GPW calculations in CP2K we use the Goedecker-Teter-Hutter (GTH) pseudopotentials (PP) to represent the core electrons.[60-61] The self-consistent cycle was converged using the orbital transformation method[62] with a direct inversion in the iterative space (DIIS) minimizer[63] and an always-stable predictor-corrector extrapolation method[64]. The electronic gradient tolerance was set to 5×10^{-7} and a cutoff of 400 Ry to represent the electron density in an auxiliary plane-wave basis was employed.

For the classical AIMD simulations, the reference forces were calculated every 0.5 fs and the full forces every 2 fs. We equilibrated the system for 6 ps using a Langevin thermostat with a time constant of 0.3 ps. We performed 200 ps production runs with a global stochastic velocity rescaling thermostat[65] with a time constant of 1 ps. For the classical AIMD simulations at T = 330 K, we used the same general settings outlined above, but we equilibrate the system for 12 ps and we perform shorter 50 ps production runs due to faster convergence at the higher temperature. At 330 K, simulations were also performed with the revPBE0-D3 density functional using a setup identical to that in previous work[4]. The data presented for revPBE0-D3 at 300K is the same as in Ref. [4]. In all the cases, we performed two independent equilibration and production runs for a total of 400 ps and 100 ps (with each functional) of production trajectory at 300 K and 330 K, respectively.

For the path integral AIMD simulations, we followed the same validated protocol employed in previous studies.[4, 34] We performed thermostatted ring polymer molecular dynamics (TRPMD)[66] with an MTS propagator[53], 32 path integral replicas and ring polymer contraction (RPC)[34, 67]. Reference forces were evaluated every 0.25 fs on all 32 replicas, while full forces were evaluated every 2 fs on the centroid using RPC. The PILE thermostat (Langevin thermostats attached to the normal modes of atomic ring polymers) was used in these simulations, as appropriate for TRPMD.[33] Two independent production runs of 100 ps each were performed.

We also performed MD simulations using the many-body water potential MB-pol.[68] All simulations were done in the NVT ensemble with 256 water molecules in a periodic cubic box of a 19.731 Å side (i.e. density of bulk water). We used the implementation and the setup of MB-pol provided by Paesani and co-workers, together with the installation and input files for i-PI. Classical simulations were performed at both 300 K and 330 K with a 0.5 fs time step and a global stochastic velocity rescaling thermostat with a time constant of 1 ps. We performed two independent production runs of 200 ps each at each temperature after at least 50 ps of equilibration in each case. We also performed a TRPMD simulation at 300 K with a time step of 0.25 fs and a total length of one production run of 200 ps. The initial condition was prepared by running a previously equilibrated configuration from classical MD with TRPMD for 5 ps. Dipole moments along these trajectories required for the calculation of IR spectra were calculated using the μ-pol model[69] as obtained from the above implementation from the authors of MB-pol.

Trajectory analysis. Using snapshots every 10 frames, we calculated the probability distributions of several standard structural metrics: the proton-sharing coordinate in hydrogen bonds ($\delta = d_{\mathrm{OH}} - d_{\mathrm{O'H}}$), the hydrogen bond angle ($\theta = \widehat{\mathrm{OHO'}}$), the covalent bond distance (d_{OH}), the molecular dipole moments calculated using the centers of the maximally-localized Wannier functions (μ), and the distance between the oxygen atom and Wannier centers (d_{OX}). For the TRPMD trajectories, these static quantities were evaluated on and averaged over all the 32 replicas. We also analyzed some standard dynamical properties such as the self-diffusivity (*D*), the vibrational density of states (VDOS), and the infrared (IR) spectrum.[70] For the analysis of dynamic quantities we use the centroid of the TRPMD trajectories. The self-diffusion coefficients *D* were calculated from the mean-squared displacement (MSD) using Einstein's diffusion equation. We divided each trajectory into 25 ps segments and performed a linear fit on the last third of each of the MSD curves. The final value of the diffusivity is calculated as the average over all the segments, and the error bars associated correspond to the standard errors. Further analysis of the size of the error bars expected in the diffusion coefficients for a given trajectory length can be found in our previous work.[4] In order to compare with experimental measurements, the diffusivity values were corrected for hydrodynamic finite-size effects on periodic systems,[71] i.e. extrapolated to the infinite bulk. We used the experimental shear viscosity of water ($\eta = 0.8925 \times 10^{-3}$ Pa · s) for these corrections. We calculated the VDOS only for the hydrogen atoms using the velocity autocorrelation function. We calculated the IR absorption spectrum from the autocorrelation

function of the total dipole moment of the simulation box[72], where the molecular dipoles were calculated using the maximally-localized Wannier orbitals, as stated earlier.

ACKNOWLEDGMENTS. THG and LRP were supported by the Director, Office of Science, Office of Basic Energy Sciences, Chem. Sciences Division of the U.S. Department of Energy under Contract No. DE-AC02-05CH11231. TEM was supported by U.S. Department of Energy, Office of Science, Office of Basic Energy Sciences under Award Number DE-SC0014437. TEM also acknowledges support from a Cottrell Scholarship from the Research Corporation for Science Advancement and the Camille Dreyfus Teacher-Scholar Awards Program. OM was supported by the grant Primus16/SCI/27/247019. This research received a 2017 ASCR Leadership Computing Challenge (ALCC) allocation at the National Energy Research Scientific Computing Center, a DOE Office of Science User Facility supported by the Office of Science of the U.S. Department of Energy under Contract No. DE-AC02-05CH11231.

REFERENCES

1. Demerdash, O.; Wang, L.-P.; Head-Gordon, T. Advanced models for water simulations. *WIRES: Comp. Mol. Sci.* **2018,** *8* (1), e1355.
2. Yao, Y.; Kanai, Y. Free Energy Profile of NaCl in Water: First-Principles Molecular Dynamics with SCAN and ωB97X-V Exchange–Correlation Functionals. *J. Chem. Theory. Comp.* **2018,** *14* (2), 884-893.
3. Ruiz Pestana, L.; Mardirossian, N.; Head-Gordon, M.; Head-Gordon, T. Ab initio molecular dynamics simulations of liquid water using high quality meta-GGA functionals. *Chem. Sci.* **2017,** *8* (5), 3554-3565.
4. Marsalek, O.; Markland, T. E. Quantum Dynamics and Spectroscopy of Ab Initio Liquid Water: The Interplay of Nuclear and Electronic Quantum Effects. *J. Phys. Chem. Lett.* **2017,** *8* (7), 1545-1551.
5. Chen, M.; Ko, H.-Y.; Remsing, R. C.; Calegari Andrade, M. F.; Santra, B.; Sun, Z.; Selloni, A.; Car, R.; Klein, M. L.; Perdew, J. P.; Wu, X. Ab initio theory and modeling of water. *Proc. Natl. Acad. Sci.***2017,** *114* (41), 10846.
6. Skinner, L. B.; Galib, M.; Fulton, J. L.; Mundy, C. J.; Parise, J. B.; Pham, V. T.; Schenter, G. K.; Benmore, C. J. The structure of liquid water up to 360 MPa from x-ray diffraction measurements using a high Q-range and from molecular simulation. *J. Chem. Phys.* **2016,** *144* (13), 134504.
7. Gaiduk, A. P.; Gygi, F.; Galli, G. Density and Compressibility of Liquid Water and Ice from First-Principles Simulations with Hybrid Functionals. *J. Phys. Chem. Lett.* **2015,** *6* (15), 2902-2908.
8. DiStasio, R. A.; Santra, B.; Li, Z.; Wu, X.; Car, R. The individual and collective effects of exact exchange and dispersion interactions on the ab initio structure of liquid water. *J. Chem. Phys.* **2014,** *141* (8), 084502.
9. Lin, I. C.; Seitsonen, A. P.; Tavernelli, I.; Rothlisberger, U. Structure and Dynamics of Liquid Water from ab Initio Molecular Dynamics—Comparison of BLYP, PBE, and revPBE

Density Functionals with and without van der Waals Corrections. *J. Chem. Theory. Comp.* **2012,** *8* (10), 3902-3910.
10. Zhang, C.; Wu, J.; Galli, G.; Gygi, F. Structural and Vibrational Properties of Liquid Water from van der Waals Density Functionals. *J. Chem. Theory. Comp.* **2011,** *7* (10), 3054-3061.
11. Del Ben, M.; Schönherr, M.; Hutter, J.; VandeVondele, J. Bulk Liquid Water at Ambient Temperature and Pressure from MP2 Theory. *J. Phys. Chem. Lett.* **2013,** *4* (21), 3753-3759.
12. Willow, S. Y.; Zeng, X. C.; Xantheas, S. S.; Kim, K. S.; Hirata, S. Why Is MP2-Water "Cooler" and "Denser" than DFT-Water? *J. Phys. Chem. Lett.* **2016,** *7* (4), 680-684.
13. Becke, A. D. Density-functional exchange-energy approximation with correct asymptotic behavior. *Phys. Rev. A* **1988,** *38* (6), 3098-3100.
14. Lee, C.; Yang, W.; Parr, R. G. Development of the Colle-Salvetti correlation-energy formula into a functional of the electron density. *Phys. Rev. B* **1988,** *37* (2), 785-789.
15. Perdew, J. P.; Burke, K.; Ernzerhof, M. Generalized Gradient Approximation Made Simple. *Phys. Rev. Lett.* **1996,** *77* (18), 3865-3868.
16. McGrath, M. J.; Siepmann, J. I.; Kuo, I. F. W.; Mundy, C. J.; VandeVondele, J.; Hutter, J.; Mohamed, F.; Krack, M. Isobaric–Isothermal Monte Carlo Simulations from First Principles: Application to Liquid Water at Ambient Conditions. *ChemPhysChem* **2005,** *6* (9), 1894-1901.
17. Kuo, I. F. W.; Mundy, C. J.; Eggimann, B. L.; McGrath, M. J.; Siepmann, J. I.; Chen, B.; Vieceli, J.; Tobias, D. J. Structure and Dynamics of the Aqueous Liquid−Vapor Interface: A Comprehensive Particle-Based Simulation Study. *J. Phys. Chem. B* **2006,** *110* (8), 3738-3746.
18. Schmidt, J.; VandeVondele, J.; Kuo, I. F. W.; Sebastiani, D.; Siepmann, J. I.; Hutter, J.; Mundy, C. J. Isobaric−Isothermal Molecular Dynamics Simulations Utilizing Density Functional Theory: An Assessment of the Structure and Density of Water at Near-Ambient Conditions. *J. Phys. Chem. B* **2009,** *113* (35), 11959-11964.
19. Perdew, J. P.; Zunger, A. Self-interaction correction to density-functional approximations for many-electron systems. *Phys. Rev. B* **1981,** *23* (10), 5048-5079.
20. Santra, B.; Michaelides, A.; Scheffler, M. Coupled cluster benchmarks of water monomers and dimers extracted from density-functional theory liquid water: The importance of monomer deformations. *J. Chem. Phys.* **2009,** *131* (12), 124509.
21. Gillan, M. J.; Manby, F. R.; Towler, M. D.; Alfè, D. Assessing the accuracy of quantum Monte Carlo and density functional theory for energetics of small water clusters. *J. Chem. Phys.* **2012,** *136* (24), 244105.
22. Markland, T. E.; Ceriotti, M. Nuclear quantum effects enter the mainstream. *Nature Rev. Chem.* **2018,** *2*, 0109.
23. Grimme, S. Semiempirical GGA-type density functional constructed with a long-range dispersion correction. *J. Comp. Chem.* **2006,** *27* (15), 1787-1799.
24. Goerigk, L.; Grimme, S. A thorough benchmark of density functional methods for general main group thermochemistry, kinetics, and noncovalent interactions. *Phys. Chem. Chem. Phys.* **2011,** *13* (14), 6670-6688.
25. Vydrov, O. A.; Van Voorhis, T. Implementation and assessment of a simple nonlocal van der Waals density functional. *J. Chem. Phys.* **2010,** *132* (16), 164113.
26. Sabatini, R.; Gorni, T.; de Gironcoli, S. Nonlocal van der Waals density functional made simple and efficient. *Phys. Rev. B* **2013,** *87* (4), 041108.
27. Dion, M.; Rydberg, H.; Schröder, E.; Langreth, D. C.; Lundqvist, B. I. Van der Waals Density Functional for General Geometries. *Phys. Rev. Lett.* **2004,** *92* (24), 246401.

28. Ferri, N.; DiStasio, R. A., Jr.; Ambrosetti, A.; Car, R.; Tkatchenko, A. Electronic properties of molecules and surfaces with a self-consistent interatomic van der Waals density functional. *Phys. Rev. Lett.* **2015,** *114* (17), 176802.
29. Tkatchenko, A.; DiStasio, R. A., Jr.; Car, R.; Scheffler, M. Accurate and efficient method for many-body van der Waals interactions. *Phys. Rev. Lett.* **2012,** *108* (23), 236402.
30. Lin, I. C.; Seitsonen, A. P.; Coutinho-Neto, M. D.; Tavernelli, I.; Rothlisberger, U. Importance of van der Waals Interactions in Liquid Water. *J. Phys. Chem. B* **2009,** *113* (4), 1127-1131.
31. Gillan, M. J.; Alfè, D.; Michaelides, A. Perspective: How good is DFT for water? *J. Chem. Phys.* **2016,** *144* (13), 130901.
32. Tuckerman, M.; Berne, B. J.; Martyna, G. J. Reversible multiple time scale molecular dynamics. *J. Chem. Phys.* **1992,** *97* (3), 1990-2001.
33. Ceriotti, M.; Parrinello, M.; Markland, T. E.; Manolopoulos, D. E. Efficient stochastic thermostatting of path integral molecular dynamics. *J. Chem. Phys.* **2010,** *133* (12), 124104.
34. Marsalek, O.; Markland, T. E. Ab initio molecular dynamics with nuclear quantum effects at classical cost: Ring polymer contraction for density functional theory. *J. Chem. Phys.* **2016,** *144* (5), 054112.
35. Remsing, R. C.; Baer, M. D.; Schenter, G. K.; Mundy, C. J.; Weeks, J. D. The Role of Broken Symmetry in Solvation of a Spherical Cavity in Classical and Quantum Water Models. *J. Phys. Chem. Lett.* **2014,** *5* (16), 2767-2774.
36. Mardirossian, N.; Ruiz Pestana, L.; Womack, J. C.; Skylaris, C.-K.; Head-Gordon, T.; Head-Gordon, M. Use of the rVV10 Nonlocal Correlation Functional in the B97M-V Density Functional: Defining B97M-rV and Related Functionals. *J. Phys. Chem. Lett.* **2017,** *8* (1), 35-40.
37. Mardirossian, N.; Head-Gordon, M. Mapping the genome of meta-generalized gradient approximation density functionals: The search for B97M-V. *J. Chem. Phys.* **2015,** *142* (7), 074111.
38. Mardirossian, N.; Head-Gordon, M. Thirty years of density functional theory in computational chemistry: an overview and extensive assessment of 200 density functionals. *Mol. Phys.* **2017,** *115* (19), 2315-2372.
39. Skinner, L. B.; Huang, C.; Schlesinger, D.; Pettersson, L. G.; Nilsson, A.; Benmore, C. J. Benchmark oxygen-oxygen pair-distribution function of ambient water from x-ray diffraction measurements with a wide Q-range. *J. Chem. Phys.* **2013,** *138* (7), 074506.
40. Soper, A. K. The Radial Distribution Functions of Water as Derived from Radiation Total Scattering Experiments: Is There Anything We Can Say for Sure? *ISRN Physical Chemistry* **2013,** *2013*, 279463.
41. Brookes, D. H.; Head-Gordon, T. Family of Oxygen–Oxygen Radial Distribution Functions for Water. *J. Phys. Chem. Lett.* **2015,** *6* (15), 2938-2943.
42. Peng, H.; Yang, Z.-H.; Perdew, J. P.; Sun, J. Versatile van der Waals Density Functional Based on a Meta-Generalized Gradient Approximation. *Phys. Rev. X* **2016,** *6* (4), 041005.
43. Wiktor, J.; Ambrosio, F.; Pasquarello, A. Note: Assessment of the SCAN+rVV10 functional for the structure of liquid water. *J. Chem. Phys.* **2017,** *147* (21), 216101.
44. Sun, J.; Ruzsinszky, A.; Perdew, J. P. Strongly Constrained and Appropriately Normed Semilocal Density Functional. *Phys. Rev. Lett.* **2015,** *115* (3), 036402.
45. Ceriotti, M.; Cuny, J.; Parrinello, M.; Manolopoulos, D. E. Nuclear quantum effects and hydrogen bond fluctuations in water. *Proc. Natl. Acad. Sci.***2013,** *110* (39), 15591-15596.

46. Habershon, S.; Markland, T. E.; Manolopoulos, D. E. Competing quantum effects in the dynamics of a flexible water model. *J. Chem. Phys.* **2009,** *131* (2), 024501.
47. Bertie, J. E.; Lan, Z. Infrared Intensities of Liquids XX: The Intensity of the OH Stretching Band of Liquid Water Revisited, and the Best Current Values of the Optical Constants of H2O(l) at 25°C between 15,000 and 1 cm−1. *Applied Spectroscopy* **1996,** *50* (8), 1047-1057.
48. Rossi, M.; Liu, H.; Paesani, F.; Bowman, J.; Ceriotti, M. Communication: On the consistency of approximate quantum dynamics simulation methods for vibrational spectra in the condensed phase. *J. Chem. Phys.* **2014,** *141* (18), 181101.
49. Holz, M.; Heil, S. R.; Sacco, A. Temperature-dependent self-diffusion coefficients of water and six selected molecular liquids for calibration in accurate 1H NMR PFG measurements. *Phys. Chem. Chem. Phys.* **2000,** *2* (20), 4740-4742.
50. Reddy, S. K.; Straight, S. C.; Bajaj, P.; Huy Pham, C.; Riera, M.; Moberg, D. R.; Morales, M. A.; Knight, C.; Götz, A. W.; Paesani, F. On the accuracy of the MB-pol many-body potential for water: Interaction energies, vibrational frequencies, and classical thermodynamic and dynamical properties from clusters to liquid water and ice. *J. Chem. Phys.* **2016,** *145* (19), 194504.
51. McGrath, M. J.; Siepmann, J. I.; Kuo, I. F. W.; Mundy, C. J. Vapor–liquid equilibria of water from first principles: comparison of density functionals and basis sets. *Mol. Phys.* **2006,** *104* (22-24), 3619-3626.
52. Ceriotti, M.; More, J.; Manolopoulos, D. E. i-PI: A Python interface for ab initio path integral molecular dynamics simulations. *Comp. Phys. Comm.* **2014,** *185* (3), 1019-1026.
53. Kapil, V.; VandeVondele, J.; Ceriotti, M. Accurate molecular dynamics and nuclear quantum effects at low cost by multiple steps in real and imaginary time: Using density functional theory to accelerate wavefunction methods. *J. Chem. Phys.* **2016,** *144* (5), 054111.
54. Hutter, J.; Iannuzzi, M.; Schiffmann, F.; VandeVondele, J. cp2k: atomistic simulations of condensed matter systems. *WIRES: Comp. Mol. Sci.* **2014,** *4* (1), 15-25.
55. Frauenheim, T.; Seifert, G.; Elsterner, M.; Hajnal, Z.; Jungnickel, G.; Porezag, D.; Suhai, S.; Scholz, R. A Self-Consistent Charge Density-Functional Based Tight-Binding Method for Predictive Materials Simulations in Physics, Chemistry and Biology. *Phys. Stat. Sol. (b)* **2000,** *217* (1), 41-62.
56. Grimme, S.; Antony, J.; Ehrlich, S.; Krieg, H. A consistent and accurate ab initio parametrization of density functional dispersion correction (DFT-D) for the 94 elements H-Pu. *J. Chem. Phys.* **2010,** *132* (15), 154104.
57. Kohn, W.; Sham, L. J. Self-Consistent Equations Including Exchange and Correlation Effects. *Phys. Rev.* **1965,** *140* (4A), A1133-A1138.
58. Lippert, G.; Hutter, J.; Parrinello, M. A hybrid Gaussian and plane wave density functional scheme. *Mol. Phys.* **1997,** *92* (3), 477-488.
59. VandeVondele, J.; Krack, M.; Mohamed, F.; Parrinello, M.; Chassaing, T.; Hutter, J. Quickstep: Fast and accurate density functional calculations using a mixed Gaussian and plane waves approach. *Comp. Phys. Comm.* **2005,** *167* (2), 103-128.
60. Goedecker, S.; Teter, M.; Hutter, J. Separable dual-space Gaussian pseudopotentials. *Phys. Rev. B* **1996,** *54* (3), 1703-1710.
61. Hartwigsen, C.; Goedecker, S.; Hutter, J. Relativistic separable dual-space Gaussian pseudopotentials from H to Rn. *Phys. Rev. B* **1998,** *58* (7), 3641-3662.
62. VandeVondele, J.; Hutter, J. An efficient orbital transformation method for electronic structure calculations. *J. Chem. Phys.* **2003,** *118* (10), 4365-4369.

63. Weber, V.; VandeVondele, J.; Hutter, J.; Niklasson, A. M. N. Direct energy functional minimization under orthogonality constraints. *J. Chem. Phys.* **2008,** *128* (8), 084113.
64. Kolafa, J. Time-reversible always stable predictor–corrector method for molecular dynamics of polarizable molecules. *J. Comp. Chem.* **2004,** *25* (3), 335-342.
65. Bussi, G.; Donadio, D.; Parrinello, M. Canonical sampling through velocity rescaling. *J. Chem. Phys.* **2007,** *126* (1), 014101.
66. Rossi, M.; Ceriotti, M.; Manolopoulos, D. E. How to remove the spurious resonances from ring polymer molecular dynamics. *J. Chem. Phys.* **2014,** *140* (23), 234116.
67. Markland, T. E.; Manolopoulos, D. E. An efficient ring polymer contraction scheme for imaginary time path integral simulations. *J. Chem. Phys.* **2008,** *129* (2), 024105.
68. Medders, G. R.; Götz, A. W.; Morales, M. A.; Bajaj, P.; Paesani, F. On the representation of many-body interactions in water. *J. Chem. Phys.* **2015,** *143* (10), 104102.
69. Medders, G. R.; Paesani, F. Infrared and Raman Spectroscopy of Liquid Water through "First-Principles" Many-Body Molecular Dynamics. *J. Chem. Theory. Comp.* **2015,** *11* (3), 1145-1154.
70. Schmitz, M.; Tavan, P. Vibrational spectra from atomic fluctuations in dynamics simulations. I. Theory, limitations, and a sample application. *J. Chem. Phys.* **2004,** *121* (24), 12233-12246.
71. Yeh, I.-C.; Hummer, G. System-Size Dependence of Diffusion Coefficients and Viscosities from Molecular Dynamics Simulations with Periodic Boundary Conditions. *J. Phys. Chem. B* **2004,** *108* (40), 15873-15879.
72. Ramírez, R.; López-Ciudad, T.; P, P. K.; Marx, D. Quantum corrections to classical time-correlation functions: Hydrogen bonding and anharmonic floppy modes. *J. Chem. Phys.* **2004,** *121* (9), 3973-3983.